Development of Artificial Skin Surface Ridges with Vibrotactile Sensing Elements for Incipient Slip Detection

Yoji Yamada, Isao Fujimoto,
Tetsuya Morizono and Yoji Umetani

Toyota Technological Institute
2-12-1, Hisakata, Tenpaku,
Nagoya 468-8511, Japan

Takashi Maeno and Daisuke Yamada

Department of Mechanical Engineering
Keio University
3-14-1, Hiyoshi, Kohoku-ku,
Yokohama 223-8522, Japan

Abstract

This paper deals with the development of artificial skin surface ridges for incipient slip detection in pursuit of elucidating the mechanism of static friction sensing. We have two design phases of developing artificial skin with vibrotactile sensing elements incorporated in the skin surface ridges, before we can reach a solution to the optimized shape, size and functions. Phase ♯1 is to examine dynamic characteristics of the sensing elements following the results from circuit simulation analysis. Phase ♯2 is to design shapes and sizes of the artificial skin using FE analysis. In the study, we select PVDF film as the transducer of the sensing elements, and verify that the PVDF film transducer connected with an amplifier displayed unique characteristics of stress-rate and stress-jerk sensing functions. The characteristics are separated by a cut-off frequency of approximately 1.2 kHz in the frequency domain. We show by both analyses and experiments that the signal obtained from the transducer circuit with the above cut-off frequency characteristics convey useful information to predict a gross slip through detection of incipient slip.

1 Introduction

Most of the conventional approaches to construction of various robot tactile sensor mechanisms hold a fundamental problem of a spatial limitation when they are attempted to be mounted on a small area of a robot fingertip for integration of their individual functions. This is because the limited space at a robot fingertip cannot house many sensor mechanisms without causing any mechanical interference with one another. By contact, a variety of human tactile perceptions are attained through integrated processing of tactile information from only several kinds of mechanoreceptors. Therefore, we consider it very important to build tactile sensing systems based upon a design policy of taking the behavior of tactile sensing elements and the tissue embedding them at the same time. Consequently, it becomes worth notice to realize artificial skin with sensing elements incorporated into the skin tissue so that they can be expected to have various robot tactile perception capabilities under a novel platform concept: The sensing elements should have a wider frequency detectable range and acquire meaningful information by their elaborate spatial allocation. In the study, we demonstrate the effectiveness of this design policy by pursuing incipient slip detection which plays an important role in elucidating the static friction sensation mechanism.

For this purpose, we decided to attain vibrotactile sensing capabilities on a skin tissue that has softness like humans. Early, Johansson et al.[1] examined in their study of human static friction sensation that a parallel change in the grip and the load forces is observed during precision grip of an object and the ratio between the two forces is adapted to result in the static friction coefficient between the finger skin surface and the object. According to their suggestion that insipient slip information should play an important role in such precision grip, several studies on robotic incipient slip detection have been reported. Gaetano et al. [2] proposed a tactile sensor system capable of detecting the incipiency of slip between an object and the sensor surface using the normal and shear stress information from arrays of PVDF transducers. They showed by both simulation and experimentation that a trained neural network with the normal and shea stress signal patterns allowed them to find the incipient slip. However, this method is different from the standard detecting method of incipient slip: An object in contact with a rubber surface is slid on a curved surface and the peripheral area of the contact is initiated to slip.

In this respect, Tremblay et al. [3] demonstrated the effectiveness of incipient slip detection more early using the peripheral slip signal from accelerometers which were mounted on a curved soft surface.

Similarly, J.S.Son et al.[4] also devised the surface of the rubber skin to have molded surface texture with arrayed tiny nibs for the purpose of easily obtaining the incipient slip. However, we can still design better shape and structure of the skin surface ridges with vibrotactile sensing elements because the mechanical behavior of nibs and the directivity of the sensors are

not necessarily optimized in the above two proposals due to their separate allocation. As the background of establishing a novel design strategy, we have studied the dynamic response of human finger skin for tactile receptors focusing on the effect of epidermal ridges using FE analysis [5]. We have also proposed to detect impulsive high-frequency vibratory signal at robotic finger surface ridges where PVDF film strips are embedded for isolating a slip phase from various other contact phases [6].

Moreover, what kind of transducers with 20 dB/dec or higher order dynamic sensing characteristics we should use is also an important technical issue. Though the above approach by Tremblay et al. to using accelerometers is considered to have higher sensitivity in acquiring vibrotactile information, they cannot be easily downsized. PVDF film transducers which were introduced to this study field by Dario et al. [7] are promising due to their flexibility and high sensitivity. Later work on texture distinguishment by Patterson et al. [8] is also notable, from the viewpoint that the work was the first proposal of using the PVDF film transducers in dynamic tactile sensing which is a widely applicable concept developed by Howe et al.[9] They also used the same PVDF film transducers referring to it as stress-rate sensor in their work on monitoring contact conditions for dextrous robot hand manipulation. It is interesting to note that a PVDF transducer has the possibility of exhibiting various frequency characteristics in connection with an amplifier [10]

In this study, we show the development process of artificial skin surface ridges in each of which a pair of PVDF film strips are incorporated. The design process is addressed in chapter 2. Examination of the PVDF transducer characteristics is intensively described in chapter 3, which is followed by the shape and size design of artificial skin as well as its mechanical behavior analysis in chapter 4. Chapter 5 demonstrates the usefulness of our proposal.

2 Design Processes of Artificial Skin

In this study, there are two processes of designing artificial skin which are schematically described in Figure 1. The first process A consists of two design phases; design #1 and #2. Design phase #1 is to examine the frequency characteristics and the sensitivity of the transducer circuit used in the artificial skin. We select PVDF film as the transducer of artificial mechanoreceptors because the film has high mechanical flexibility and we can expect high sensitivity of piezoelectricity with dynamic responses of technical interest [9]. We consider that this phase of determining the equivalent circuit of the PVDF film in connection with an amplifier is important for later use of designing more desired PVDF transducer circuit. In design phase #2, we design the shape and size of the artificial skin. In this phase, it is important to identify where the PVDF transducers are localized and what kind of tactile information from the transducers is significant in detecting the incipient slip. The above two design phases are conducted independently, and reconsidered after taking the other phase into account as the second process to find the optimal design solution to the artificial skin with highly sensitive and reliable incipient slip detection capability.

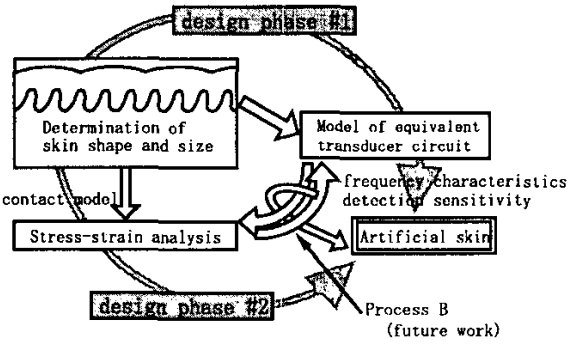

Figure 1: Design process of artificial skin

3 Design Phase]1: Examination of the PVDF Circuit Frequency Characteristic

3.1 Experimental setup

Figure 2 is the circuit that we made for our study. A differential amplifier, which is mainly a high input impedance operational amplifier, OP amp, and plays an important role of rejecting common mode noise, is connected to a PVDF film transducer. Hereafter, a PVDF film transducer followed by a differential amplifier is termed a PVDF circuit.

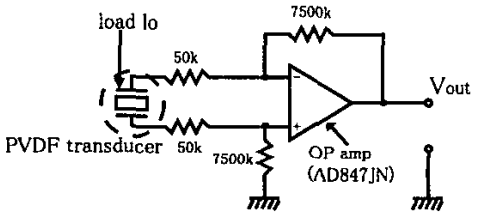

Figure 2: Circuit diagram of a PVDF circuit (a PVDF transducer + a differential amplifier)

A load lo is applied to the PVDF film transducer. It generates electric charges which are converted to output voltage v_{out} by the succeeding differential amplifier. We can monitor the two parameters lo and v_{out}, and compute the *gain* of the linear PVDF circuit system which is defined as

$$Gain = 20log|\frac{v_{out}}{lo}| \quad (1)$$

where $Gain$ is a function of frequency $f = \frac{\omega}{2\cdot}$, because the PVDF circuit exhibits a dynamic characteristic due to the parallel-series resonant property of the PVDF film and the input capacitance of the OP

amp. The experimental setup for examining the frequency characteristic of the PVDF circuit is shown in Figure 3. The PVDF transducer is preloaded at 25 N between the indentor of a vibrator and a force sensor probe. The radius of the circular contact area between the film surface and the indentor is 1.95 mm. The vibrator is driven by a sinusoidal input signal. The magnitude of the sinusoidal load lo is observed by a force sensor, and is kept constant regardless of the input frequency f which ranges from 10 to 20000 Hz.

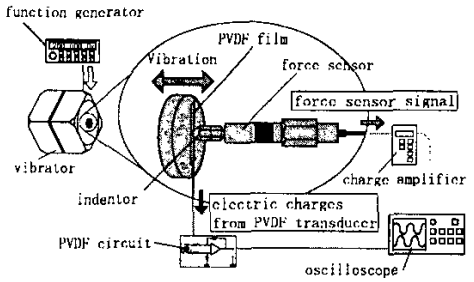

Figure 3: Experimental setup for examining the frequency characteristic of a PVDF circuit

3.2 Experimental result

The experimental result is shown in Figure 4. We should note the following three points concerning the result: (i) First order (20 dB/dec) frequency characteristic is maintained until a characteristic cut-off frequency f_c which is observed to be approximately 1.2 kHz in the frequency domain. (ii) Then, the slope is changed to the third order (60 dB/dec). We call this stress-jerk sensing characteristic in the study, we can conclude that the PVDF circuit exhibits not only stress-rate frequency characteristic which was originally pointed out by Howe et al.[9] but also stress-jerk characteristic which has never been examined before. (iii) We can observe a rapid drop at f =9 kHz. We have already traced the cause that the drop resulted from mechanical resonance of the system comprising the vibrator indentor and the PVDF film.

3.3 PVDF circuit model

In order to analyze the actual frequency characteristic in Figure 4, we propose to apply a parallel-series resonant circuit model to the PVDF transducer as an equivalent circuit. Figure 5 shows the overall equivalent circuit diagram including that of the succeeding OP amp[11].

Electric charges q_{PV} induced at the electrodes of the polarized PVDF transducer due to the applied stress results from free electrons existing in the vicinity of the electrodes. q_{PV} is proportional to the applied stress lo,

$$q_{PV} = d_{33} lo \tag{2}$$

where d_{33} is the piezoelectric strain constant: d_{33} means the ratio of the charges generated in the 3-axis (in the direction of film thickness) when a mechanical

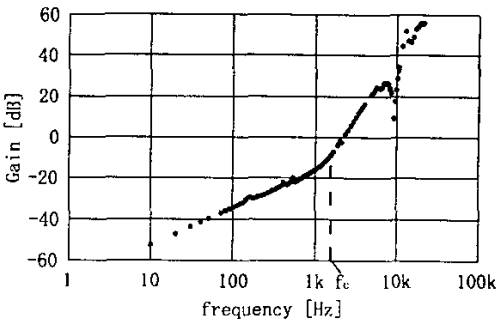

Figure 4: Experimental result

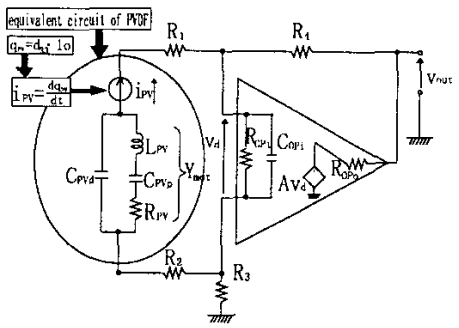

Figure 5: Overall equivalent circuit of the PVDF circuit

stress is applied to the same 3-axis. Electric current i_{PV} is obtained by computing the derivative of q_{PV}, i.e.

$$i_{PV} = \frac{dq_{PV}}{dt} \tag{3}$$

We can derive the following equations for the unknown node currents $i_n (n = 1, 2, 3, 4)$ applying Kirchhoff's voltage law and using other constant circuit parameters defined in Figure 6:

$$\frac{i_1}{j\omega C_{PVd}} + \frac{i_1 - i_2}{Y_{mot}} = 0 \tag{4}$$

$$\frac{i_2 - i_1}{Y_{mot}} + (R_1 + R_2) i_2 + R_{OPi}(i_2 - i_3) = 0 \tag{5}$$

$$R_{OPi}(i_3 - i_2) + \frac{i_3 - i_4}{j\omega C_{OPi}} = 0 \tag{6}$$

$$\frac{i_4 - i_3}{j\omega C_{OPi}} + (R_3 + R_4 + R_{OPo}) i_4 - A v_d = 0 \tag{7}$$

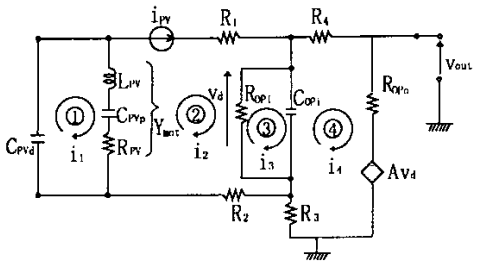

Figure 6: PVDF circuit modeling for computing *Gain* defined in (1)

$$v_d = R_{OPi}(i_3 - i_2) \tag{8}$$

$$v_{out} = Av_d - R_{OPo}\, i_4 \tag{9}$$

Solving the linear simultaneous equations (4) through (9), the PVDF circuit gain defined in (1) is formulated as

$$Gain = 20log|(\frac{1}{A_4} - R_{OPo})\frac{d_{33}j\omega e^{j\omega t}}{A_3 A_2}| \tag{10}$$

where A_2 through A_4 in formula (10) are developed as follows.

$$A_2 = \frac{Y_{mot}R_{OPi}}{1 + Y_{mot}(R_1 + R_2) + Y_{mot}R_{OPi} - A_1} \tag{11}$$

$$A_3 = \frac{1}{1 + j\omega C_{OPi}R_{OPi} - A_2} \tag{12}$$

$$A_4 = \frac{j\omega C_{OPi}}{1 + j\omega C_{OPi}(R_3 + R_4 + R_{OPo}) - A_3} \tag{13}$$

where A_1 is:

$$A_1 = \frac{j\omega C_{PVd}}{Y_{mot} + j\omega C_{PVd}} \tag{14}$$

Finally, Gain obtained from (10) through (14) is plotted as the dotted line in Figure 7.

For comparison, the experimental result of *Gain* which has been already shown in Figure 4 is again plotted in the same Figure 7. From the two characteristic curves, we conclude that the PVDF circuit can be modeled as shown in Figure 6 and the circuit gain is characteristic of having both stress-rate and stress-jerk properties.

In the PVDF circuit model, the series resonance circuit component affects the magnitude of *Gain* while the OP amp input impedance shifts f_c. These simulation results lead to a conclusion that it is necessary to analyze the PVDF circuit *Gain* characteristic by combining the PVDF transducer with the input impedance of the succeeding circuit (the differential amplifier in our study).

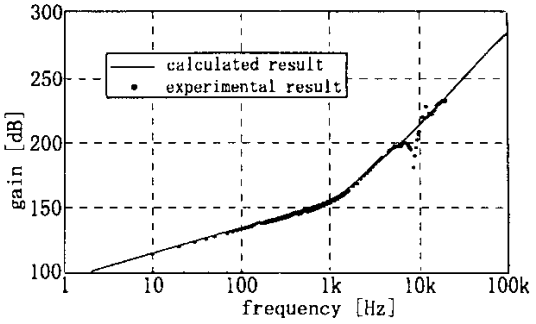

Figure 7: Computed result of Gain (166 dB is added to the experimental result in order to match the computed characteristic.)

4 Design Phase]2: Structure Design and Behavior Analysis of Artificial Skin

4.1 Shape and size design for artificial skin

A human hand can grasp an object by voluntary lifting speed of the fingers, even when the weight of the object or the friction coefficient between the fingers and the object is unknown. In the stage of designing artificial skin, we analyzed the mechanical behaviour of the skin of a human finger with surface ridges [12]. The artificial finger skin can be designed by imitating the characteristics of human fingers as follows: First, the tissue of a human finger except for bones consists of flexible materials. The material transforms contact information to the tactile receptors through elastic deformation of tissues. Second, a human finger has curved surface in broad perspective. Third, epidermal ridges are distributed at the finger surface. A pair of FA1 receptors is located at the top dermis papilla underneath one epidermal ridge.

Incipient slip easily occurs at the edge of the contact area between the artificial skin surface and an object because the surface is geometrically curved. When the incipient slip occurs, elastic deformation is suddenly reduced at the ridges located at the edge of the contact area. The motion speed of the ridges is supposed to be constant which depends on the natural frequency of the ridge, even when the friction coefficient between the skin surface and the object, and the applied force change.

A pair of FA1 receptors are located near the border between the epidermis and dermis underneath the epidermal ridge [13]. A stress concentration occurs at the location of FA1 receptors. A stress distribution inside the ridges is closely related to the deformation of ridges as shown in Figure 8. The stress exerted at the location of the paired FA1 receptors is considered to be symmetrically equal only when the normal force F_n is applied to the ridge summit as shown in Figure 8(a). However, the stress at the pair of FA1 receptors

differs each other when both F_n and the tangential force component F_t are applied to the ridge as shown in Figure 8(b). If the two stress components at the pair of FA1 receptors are subtracted, the resultant value is zero when only F_n is applied as in Figure 8(a). However the subtracted value is not zero when the external force contains not only F_n but also F_t. Particularly, when the incipient slip occurs, a velocity of the subtracted value is sharply decreased in the direction. It is expected that the incipient slip can be detected for gross slip prevention even when the friction coefficient of the object is unknown.

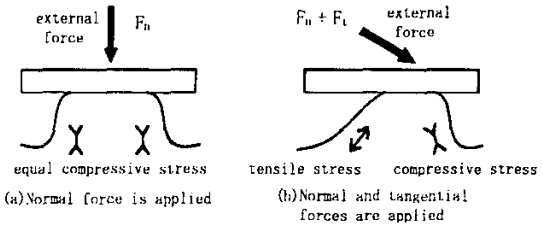

Figure 8: Destribution of stress inside the ridge

The artificial skin is designed in detail in consideration of the above mentioned characteristics of human skin: First, the shape of ridges is determined. Second, locations and directions to acquire the paired stress information inside the ridge are determined. Third, the radius of curvature for the artificial skin surface is decided. It is analyzed by FEM that all of the nine ridges contact a flat object when the normal force of 4 N is applied. The weight is about 4 N when the static friction coefficient is 1.0. Artificial skin is designed from the above conditions as shown in Figure 9.

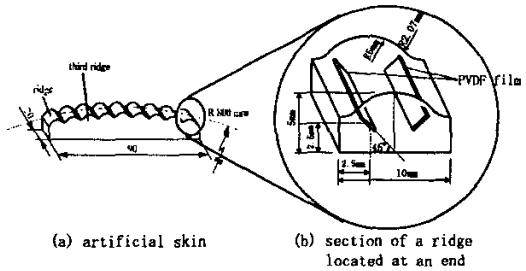

Figure 9: Design of artificial skin

4.2 Simulation of detecting incipient slip

When an external force consisting of a normal and tangential force components, F_n and F_t respectively, is applied to the artificial skin as designed in Figure 9, the differential stress signal which is computed from the stresses at S_1 and S_2 in Figure 10 is analyzed using FEM. The external force is applied as shown in Figure 11. Only the normal force is applied at first for avoiding gross slip. Then, the tangential are increased. Partial incipient slip nearly occurs from time step 200 to 300, because the divided value F_t/F_n is close to the static friction coefficient. On the other hand, the partial incipient slip does not easily occur from step 300 because the divided value F_t/F_n is considerably smaller than the static friction coefficient. Finally, the partial incipient slip easily occurs again from time step 450 toward the gross slip. All the time is divided into 550 steps. Time of one step is $1.0 \cdot 10^{-6}$ s. The computed stress-rate and stress-jerk components in the third ridge from an end are shown in Figure 12 and Figure 13, respectively. The change of the differential stress is described when incipient slip occurs in the third ridge: First, the differential stress-rate increases gradually after the lifting force starts to be added. Second, when gross slip occurs in the third ridge, the differential stress-rate signal suddenly decreases at step 450 in Figure12, and the differential stress-jerk component attains a peak value at the same step 450 in Figure 13.

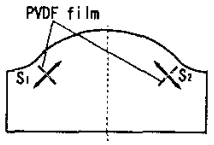

Figure 10: Points and directions for substracting the stress

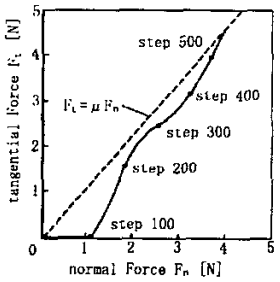

Figure 11: History of external force

It is suggested from the analysis that predicting gross slip is possible using the stress-rate and stress-jerk signals obtained in the artificial skin. Consequently, it is evident that PVDF transducers are useful for the gross slip detection because a PVDF circuit has the characteristics of stress-rate and stress-jerk as has been examined already. That is, we can use the differential information of the stress-rate and stress-jerk from the PVDF circuits.

We conducted the second experiment of verifying that the simulated results of the FE analysis for incipient slip detection could be practically observed when using the manufactured artificial skin piece in Figure 9. The experimental setup is shown in Figure 14. As

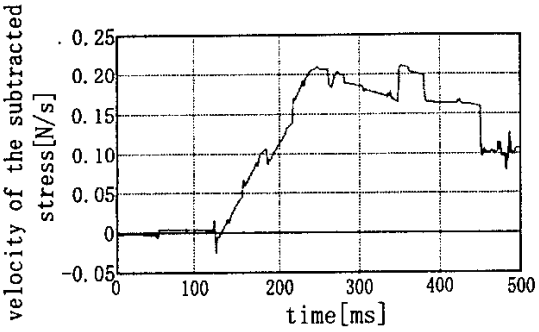

Figure 12: Velocity of the substracted stress inside third ridge

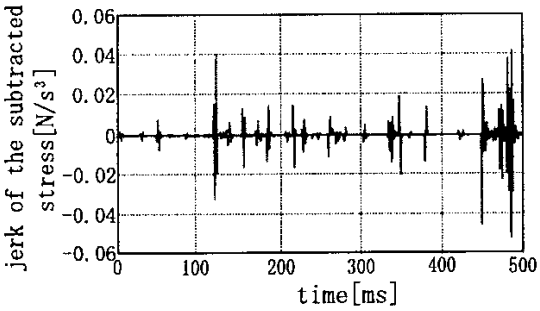

Figure 13: Jerk of the substracted stress inside third ridge

shown in the figure, artificial skin is fixed to a block plate which is driven in the x and z directions by a x-z stage. The skin is sensitive to the slip incipiency in the x direction. Two pairs of vibrotactile sensing elements made of PVDF film sheets are inserted in the second and the third ridges from a side. The aluminum plate which is in contact with the skin surface at a constant normal force is slid in the x direction. Two channels of the output voltage signals from the third element are monitored at 650 Hz sampling rate.

The differential signal v_d which is obtained by subtracting S_1 output difference from S_2 output is depicted in Figure 15. In phase P_A of the figure, low-frequency differential stress-rate signal is observed which contains a small drop component at about 160 steps. The signal profile appears to be very similar to that of the simulated result in Figure 12. The drop of the signal results from the incipient slip occurred in the ridge located next to the third. Phase P_B is the period when the incipient slip occurred in the ridge. The artificial skin can grasp the incipient slip phenomenon even though the low-frequency component in the time variation of the signal before the incipient slip and the impulsive signal component telling the incipiency of the slip are superposed. It comes from the combined stress-rate and stress-jerk sensing

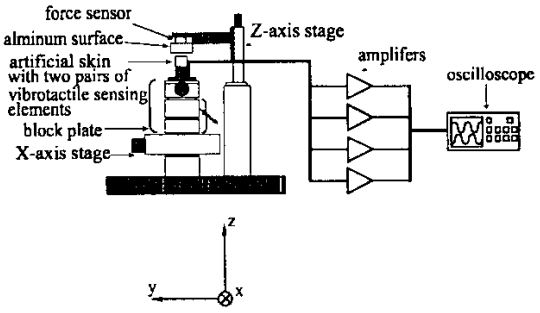

Figure 14: Experimental setup

characteristics of the PVDF circuit. We obtained the same experimental result as shown in Figure 15.

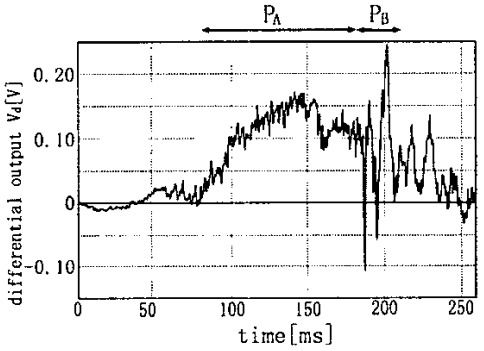

Figure 15: Experimental result

5 Conclusions

In the paper, we described the development of artificial skin with vibrotactile sensing elements based upon our design policy of considering the skin shape, location of the sensing elements, and their detectable frequency band width at the same time. We showed the design process of artificial skin, which was followed by the detailed design phases for attaining incipient slip detection. Phase ♯1 in the first process examined that a PVDF circuit, which we built as the transducer circuit had unique characteristics of stress-rate and stress-jerk. The cut-off frequency separating the two characteristics in the frequency domain was observed to be 1.2 kHz. In the design phase ♯2, we verified incipient slip detection on the curved skin surface with ridges where the differential stress-rate signal computed from the output data obtained at two points in the third ridge increased gradually. When gross slip at the ridge occurred, the differential stress-rate signal suddenly dropped and accordingly, impulsive differential stress-jerk signals were generated. The above verification in the first design process showed that the

sensor could predict a gross slip of the artificial skin surface from incipient slip detection.

Our ongoing work for the second design process should include separately extracting the two kinds of differential stress signals: stress-rate and stress-jerk components which cannot isolate each other at the present stage. It is also interesting to devise a transducer circuit of the PVDF film which would allow us to detect the stress itself.

Acknowledgments

This study was supported by the Ministry of Education, Culture, Sports, Science and Technology under Grant-in-Aid for Scientific Reseach No.10450161.

References

[1] R.S.Johansson et.al.: Tactile sensory cording in the glabrous skin of the human hand, *Trends in NeuroSciences* ,Vol.6, No.1, pp27–32, 1983.

[2] G. Canepa et.al.: Detection of Incipient Object Slippage by Skin-Like Sensing and Neural Network Processing, *IEEE Transactions on Systems, Man, and Cybernetics-Part B: Cybernetics*, Vol.28, No.3, pp.348–356, 1998.

[3] Marc R. Trembly et.al.: Estimating friction using incipient slip sensing during a manipulation task, *IEEE International conference on robotics and automation*, pp.429–434, 1993.

[4] J. S. Son et al.: A Tactile Sensor for Localizing Transient Events in Manipulation, *Proceedings of 1994 Int. Conf. on Robotics and Automation*, pp.471–476, 1994.

[5] T. Maeno et al.: FE Analysis of the Dynamic Characteristics of the Human Finger Pad in Contact with Objects with/without Surface Roughness, *Proc. 1998 ASME International Mechanical Engineering Congress and Exposition*, DSC-Vol.64, pp.279–286, 1998.

[6] Y.Yamada et.al.: Slip phase isolating : impulsive signal generating vibrotactile sensor and its application to real-time object regrip control, *Robotica*, Vol.18, pp.43–49, 2000.

[7] P.Dario et.al.: Piezoelectric Polymers: New Sensor Materials for Robotic Applications, *13th International Symposium on Industrial Robots and Robots 7*, Vol.2, pp.14-34–14-49, 1983.

[8] R.W. Patterson et.al.: The induced vibration touch sensor – a new dynamic touch sensing concept , *Robotica*, Vol.4, pp.27–31, 1986.

[9] R.D.Howe et.al.: Dynamic tactile sensing: Perception of fine surface features with stress rate sensing, *IEEE transactions on robotics and automation*, Vol.9, No.2, pp.140–151, 1993.

[10] Y. Yamada et al.: Primary Development of Viscoelastic Robot Skin with Vibrotactile Sensation of Pacinian/ Non-Pachinian Channels, *Proceeding of the 3rd International Conference on Advanced Mechatronics*, pp.879–885, 1998.

[11] Sergio Franco: *Design with Operational Amplifiers and Analog Integrated Circuits*, pp.28–33, *McGraw-Hill Book Company*, 1988

[12] D.Yamada et.al.: Design of Artificial Finger Skin Having Ridges and Distributer Tactile Sensors, *32nd ISR*,pp.1243–1248, 2001.

[13] Delcomyn. Fred: *Foundation of Neurobiology. '97, W.H.Freeman*, 1997